Hierarchical Honeycomb-Structured Pd/MgO/Mg Catalyst via Microplasma Electrolytic Oxidation and Cathodic Etching for Efficient Green Oxidation of Hydrosilanes

Jun Zhou,[*a] Yue Yin,[a] Zhao-Dong Li,[a] MengYu Wang,[a] Sitong Liu,[a] Minghao Wu,[a] Xiao-Qing Cao,[b*] Junchao Ma,[c] Song Li,[a] Gao-Wu Qin[*a,d]

a. Key Laboratory for Anisotropy and Texture of Materials, School of Materials Science and Engineering, Northeastern University, Shenyang 110819, China.
b .School of Materials Science and Engineering, Peking University, Beijing, 100871, China.
c. Characteristic Laboratory of Forensic Science in Universities of Shandong Province, Shandong University of Political Science and Law, Jinan 250014, Shandong Province, China
d. Shenyang University of Chemical Technology, Shenyang 110142, China.

E-mail: hafouniu@163.com, caoxiaoqingfly@163.com, qingw@smm.neu.edu.cn

Experimental and Characterization

Synthesis of Pd/MgO/Mg-1 Catalyst

A solution was prepared by sequentially dissolving $Na_2SiO_3 \cdot 9H_2O$, KF, and KOH in 500 mL of ultrapure water, achieving concentrations of 8 g/L, 5 g/L, and 7 g/L, respectively. The mixture was stirred with a glass rod until the solution became clear and free from any visible precipitates, and then set aside. To this electrolyte, 2 mL of $PdCl_2$ solution (concentration 0.02 g/mL) was added, and the resulting mixture was stirred thoroughly to ensure homogeneity. The stirring speed was then adjusted to 500 rpm.

The electrochemical setup consisted of a steel plate as the cathode and a magnesium (Mg) plate, with dimensions 2 cm × 4 cm × 2 mm, as the anode. These were connected to the corresponding electrodes of the microplasma electrolysis oxidation device. The steel plate and Mg anode were arranged parallel to each other and placed perpendicularly in the electrolyte solution within the beaker, ensuring complete immersion. The microplasma electrolysis oxidation was conducted under constant current mode, with the following parameters: pulse frequency of 300 Hz, pulse width of 67 μs, duty cycle of 20%, and a current of 0.4 A. The device was operated for a predetermined time (e.g., 6 s), after which the power was turned off. Subsequently, the Mg anode was carefully removed, washed thoroughly with deionized water, gently dried, and then subjected to thermal treatment in a tubular furnace under a hydrogen/argon mixed atmosphere at 400°C for 2 hours. Upon completion of the heat treatment, the resulting catalyst was sealed under vacuum, thereby yielding the Pd/MgO/Mg-1 catalyst.

Synthesis of Pd/MgO/Mg-2 Catalyst

5.05 g of KNO_3 was dissolved in 500 mL of ultrapure water in a 1000 mL beaker under constant stirring with a glass rod, until a clear, transparent solution free of visible precipitates was obtained. A steel plate was employed as the anode, and the synthesized Pd/MgO/Mg-1 catalyst was used as the cathode, both of which were connected to the respective terminals of a DC power supply. The steel plate and Mg-based cathode were arranged parallel and placed perpendicularly within the electrolyte, ensuring complete immersion of both electrodes.

Catalyst Characterization:

The surface morphology of the catalyst was examined using field emission scanning electron microscopy (SEM, model: SU8010). The samples were cut into approximately 3 mm × 3 mm × 2 mm pieces, gold-coated, and analyzed for their structure and composition using energy dispersive X-ray spectroscopy (EDS). To further investigate the surface chemical composition of the catalyst, X-ray diffraction (XRD, model: Smartlab) was performed. The XRD measurements were carried out with Cu-Kα radiation (λ = 1.5406 Å), an operating voltage of 40 kV, a current of 200 mA, and a power of 18 kW. The scan was conducted in continuous mode with a scan range of 20° to 80° and a scan speed of 4°/min.

The wettability of the catalyst surface was evaluated by contact angle measurements using a contact angle goniometer (model: SL200KS). A 4 μL droplet of ultrapure water was placed on the catalyst surface using the sessile drop method, and the contact angle was measured after 10 seconds, once the droplet had fully settled. Five measurements were taken at different locations on each sample, and the average value was calculated.

Surface roughness was characterized using a laser scanning confocal microscope (model: OLS3100), with a 20× objective lens. Measurements were performed at five different points on each sample, and the average roughness was determined.

The particle size and distribution of the active components in the catalyst were analyzed using transmission electron microscopy (TEM, model: JEOL ARM200F). A focused ion beam (FIB) technique was employed to prepare the sample for TEM analysis, and high-angle annular dark-field (HAADF) imaging was conducted to obtain detailed information about the size and distribution of the active particles.

To determine the chemical composition and oxidation state of the surface-active species, X-ray photoelectron spectroscopy (XPS, model: ESCALAB 250Xi, Thermo Fisher Scientific) was used. The catalyst samples were scraped and powdered, and the XPS analysis allowed for the identification of the surface chemical states and elemental composition.

Finally, the Pd content in the catalyst was quantified by inductively coupled plasma atomic emission spectroscopy (ICP-AES, model: Avio500). The Pd/MgO layer on the catalyst surface was scraped, and the resulting sample was analyzed to precisely determine the Pd content.

Catalytic Performance Testing:

The catalytic performance of the catalyst was evaluated by its ability to catalyze the conversion of silane to silanol. The reaction mixture consisted of 20 mL acetone, 500 μL ultrapure water, and 100 μL silane, with acetone serving as the solvent. The reaction was carried out at 35°C with a stirring speed of 1500 rpm, and oxygen was continuously introduced at a flow rate of 1 mL/min. Every 15 minutes, 500 μL of the reaction mixture was withdrawn and transferred into a 2 mL volumetric flask, followed by dilution with acetone for subsequent gas chromatography (GC) analysis.

GC analysis was performed using an HP-5 column and a flame ionization detector (FID), with the detector temperature set to 280°C. The initial column temperature was set to 40°C and then ramped at a rate of 20°C/min to a final temperature of 220°C. Manual injection was performed using a micro-syringe, with 2 μL of the sample injected at each interval, and the program was run for 10 minutes. The chromatographic peak areas were recorded, and the results were used to calculate the data for each reaction time point.

The silane conversion rate, silanol yield, and catalytic turnover frequency (TOF) were calculated based on the peak areas of the internal standard, reactant, product, and by-products. The TOF value, representing the number of product moles generated per unit time by the catalyst, was calculated using the following formula:

$$TOF=n_A \times B / n_{Pd} \times t$$

where n_A is the molar amount of silane (mol), B is the silanol yield (%), n_{Pd} is the molar amount of Pd (mol), and t is the reaction time (hours).

Table S1 Pd content in Pd/MgO/Mg-1 catalyst prepared by PEO process with different times.

t (s)	10	**20**	30	120
ICP(μg/t)	4.01	**5.22**	7.07	23.30

Table S2 Pd content in Pd/MgO/Mg-2 catalyst after treating by cathode etching with different electrolyte concentrations.

Concentrations (mol/L)	0.1	**0.2**	0.4	0.8
ICP(μg/t)	6.14	**7.23**	7.31	7.03

Table S3 Pd content in Pd/MgO/Mg-2 catalyst after treating by cathode etching with different electrolytes temperature.

Temperature (℃)	**18**	25	32	39
ICP(μg/t)	**6.50**	6.36	6.66	6.87

Table S4 Pd content in Pd/MgO/Mg-2 catalyst after treating by cathode etching with different times.

Time (h)	0.5	**1.0**	1.5	2.0
ICP(μg/t)	7.12	**7.23**	6.84	5.73

Table S5 Pd content in Pd/MgO/Mg-2 catalyst after treating by cathode etching with different currents.

Current (A/m^2)	**62.5**	125	250	625
ICP(μg/t)	**6.50**	6.79	5.97	5.48

Table S6 Reaction conditions for different concentrations of dimethylphenylsilane.

	acetone	silane	C_8H_{10}	H_2O	T	rate	time	atmosphere	n_{H2O}:n_{silane}
	mL	μL	μL	μL	℃	rpm	h		
1	20	100(0.46 wt.%)	48	500	30	1500	1	O_2	42:1
2	20	200(0.90 wt.%)	96	500	30	1500	2	O_2	21:1
3	**20**	**300(1.35 wt.%)**	**144**	**500**	**30**	**1500**	**2**	**O_2**	**14:1**
4	20	500(2.22 wt.%)	240	500	30	1500	2.5	O_2	8.4:1
5	20	800(3.48 wt.%)	384	500	30	1500	2.5	O_2	8.5:1

Table S7 Reaction conditions of different oxidation conditions on silane oxidation.

number	oxidation conditions

1	**O_2+H_2O**
2	O_2
3	H_2O
4	-

Table S8 CO chemisorption results of Pd/MgO/Mg catalysts before and after etching.

Sample	Treatment	CO uptake (mmol g^{-1}_cat)	Pd surface area (m^2 g^{-1}_Pd)
Pd/MgO/Mg-1	original	≈0 (below detection limit)	≈0
Pd/MgO/Mg-2	etching	6.35×10^{-4}	3.01

Table S9 Oxidation of a series of silanes with Pd/MgO/Mg-2.

Substrate	C (wt.%)	t (min)	Conversion (%)	TOF (h^{-1})
Et_3SiH	**0.46**	**45**	**98**	**23175**
$phMe_2SiH$	1.35	60	100	15561
t- $BuMe_2SiH$	0.46	120	10	2383
iPr_3SiH	0.46	120	<1	853
Ph_3SiH	0.46	120	1	133

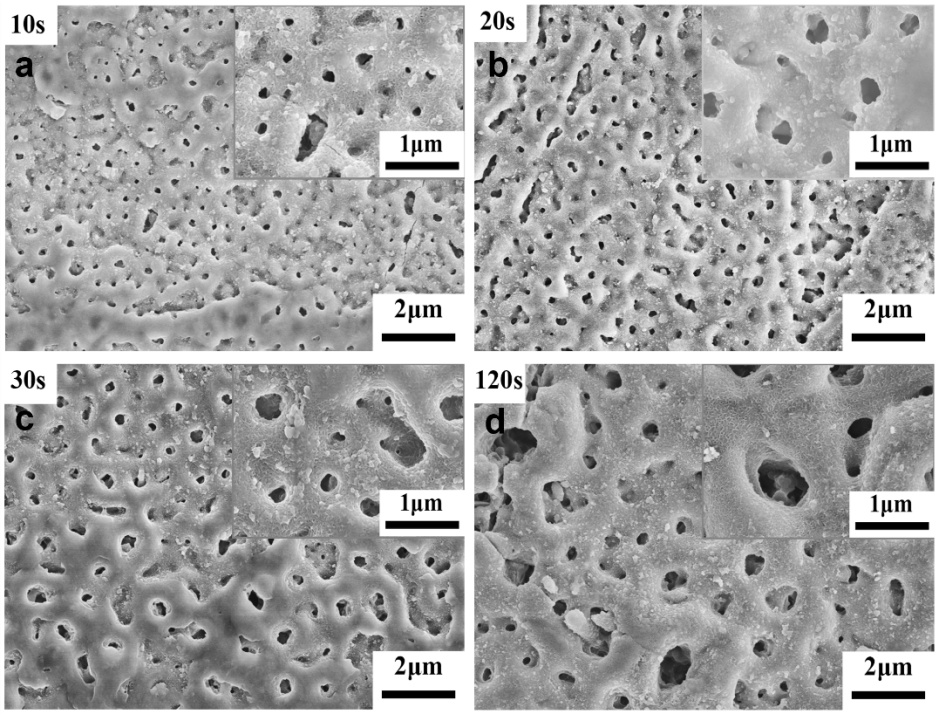

Figure S1 SEM images of Pd/MgO/Mg-1 catalyst prepared by the different PEO times. (a) 10s (b) 20s (c) 30s (d) 120s

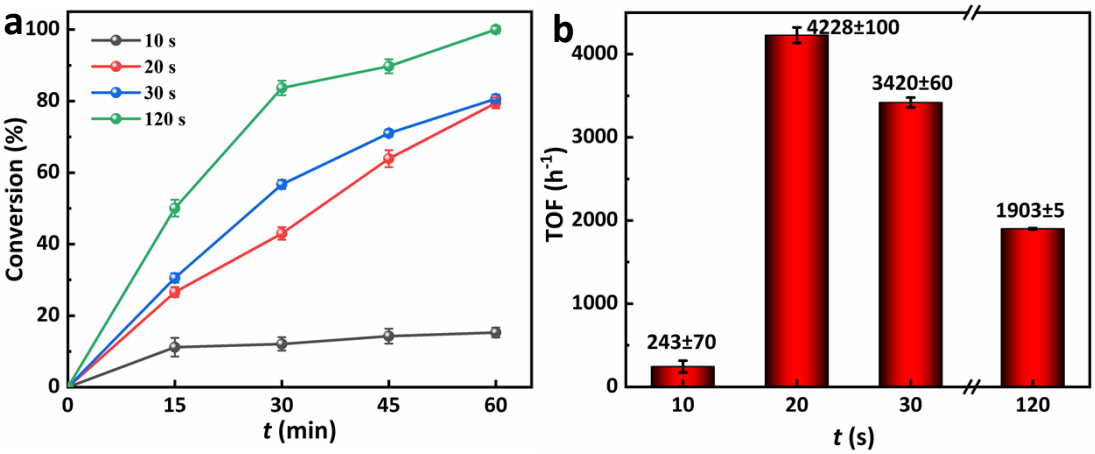

Figure S2 Comparison of the silane oxidation activity of Pd/MgO/Mg-1 prepared with different MPEO times. (a) Conversion *vs* time; (b) TOF value.

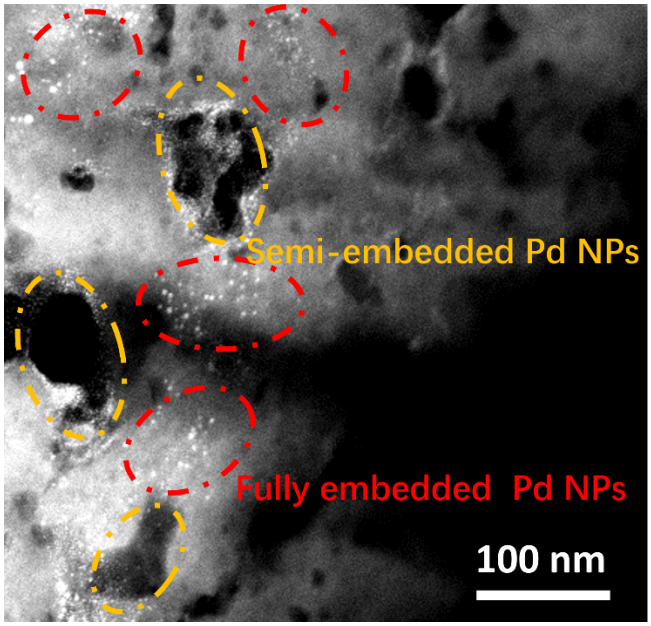

Figure S3 HAADF-STEM image of the cross-section of the Pd/MgO/Mg-2.

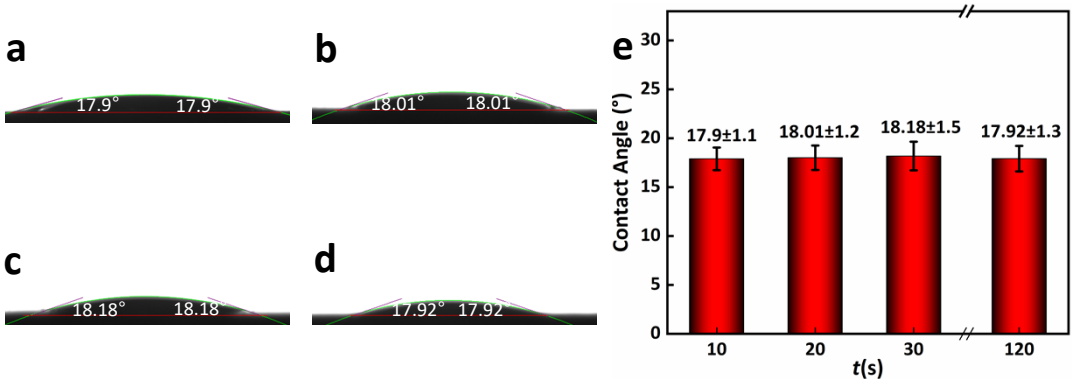

Figure S4 Contact angle of Pd/MgO/Mg-1 prepared by different MPEO time

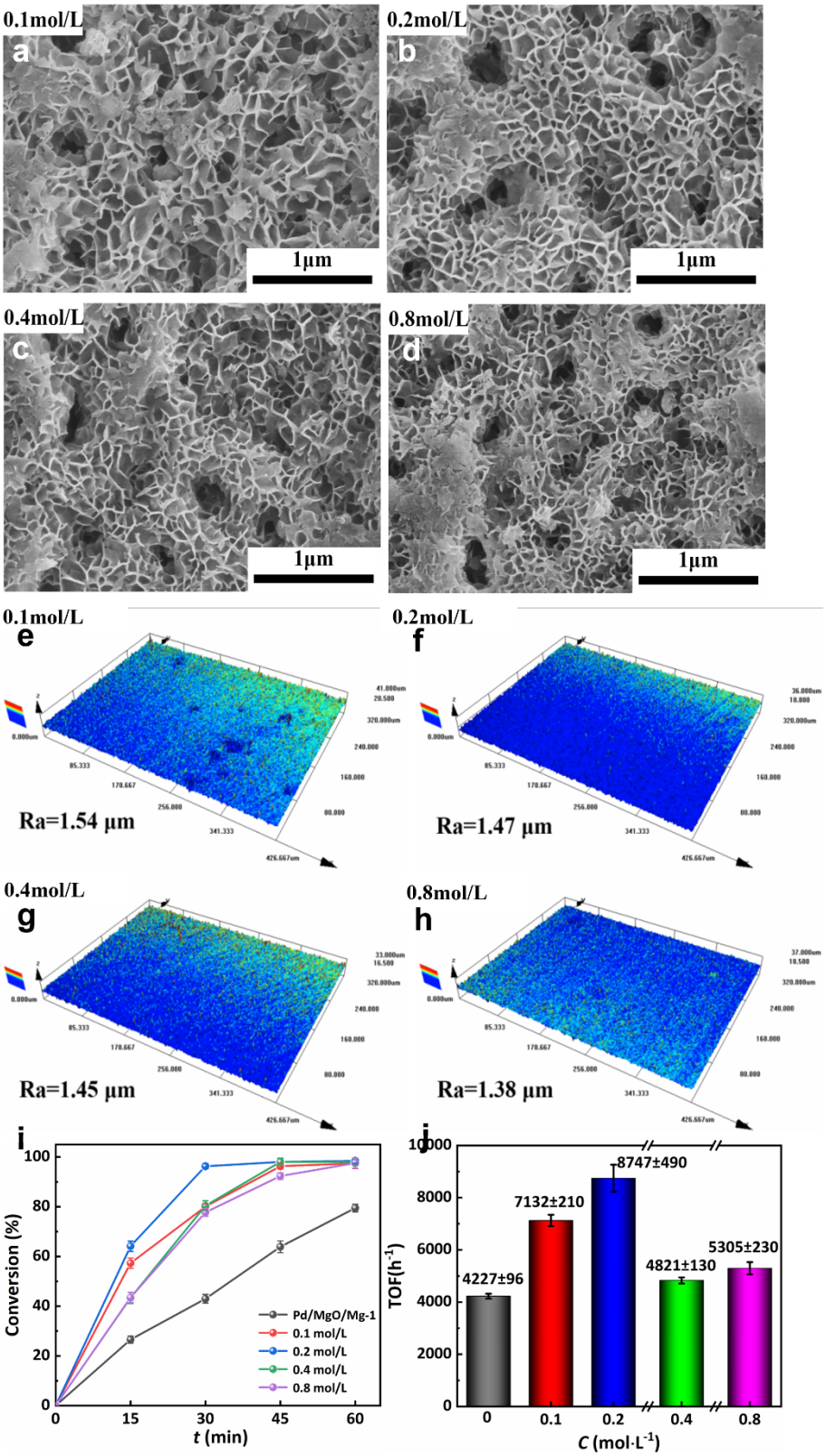

Figure S5 (a-h) Comparison of surface morphologies and roughness of Pd/MgO/Mg-2 after etching with different electrolyte concentrations;(j) Catalytic conversion; (k) TOF *vs* C.

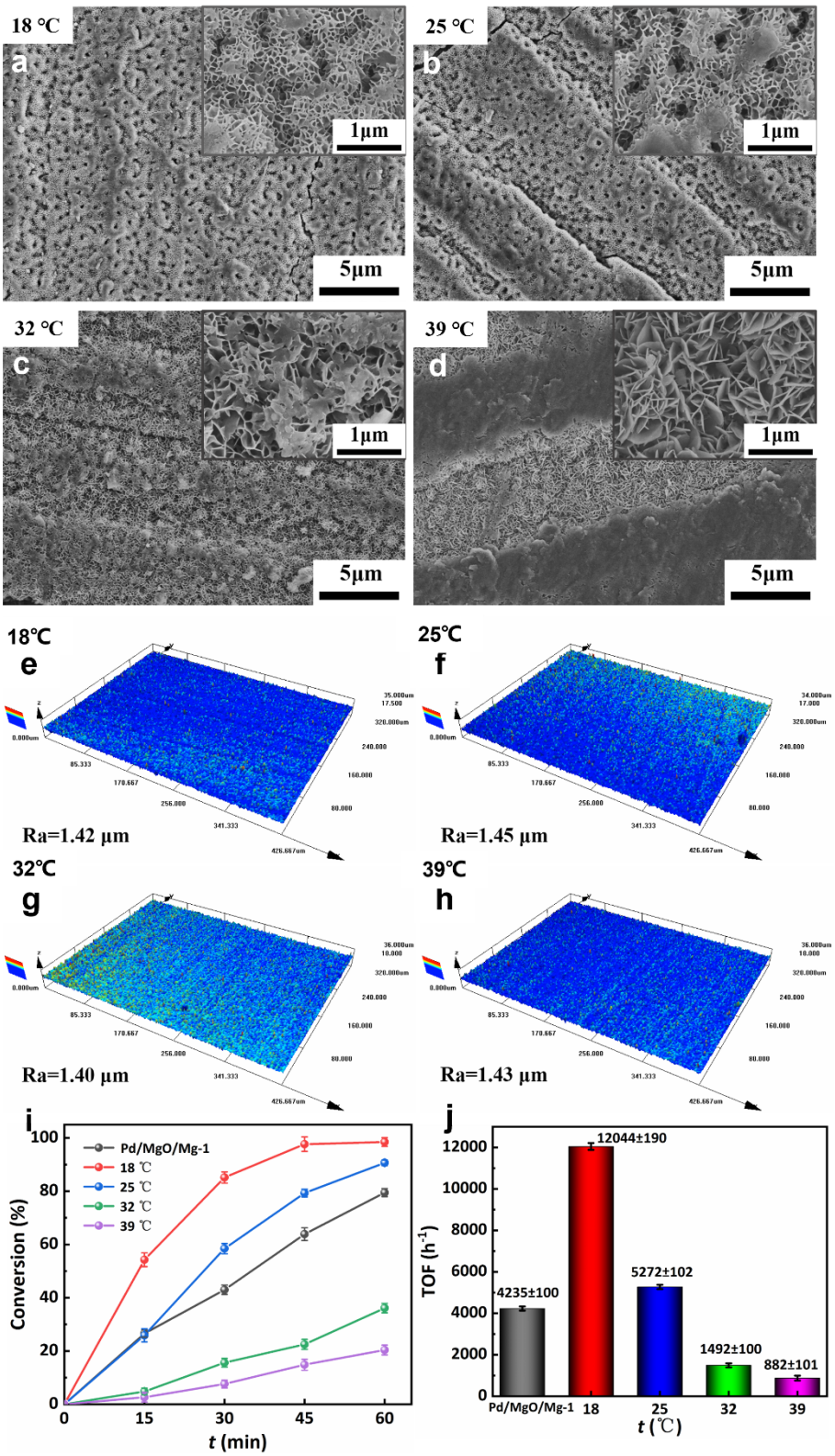

Figure S6 (a-h) Comparison of surface morphologies and roughness of Pd/MgO/Mg-2 after etching with different electrolyte temperatures; (i) Catalytic conversion; (k) TOF *vs* temperatures.

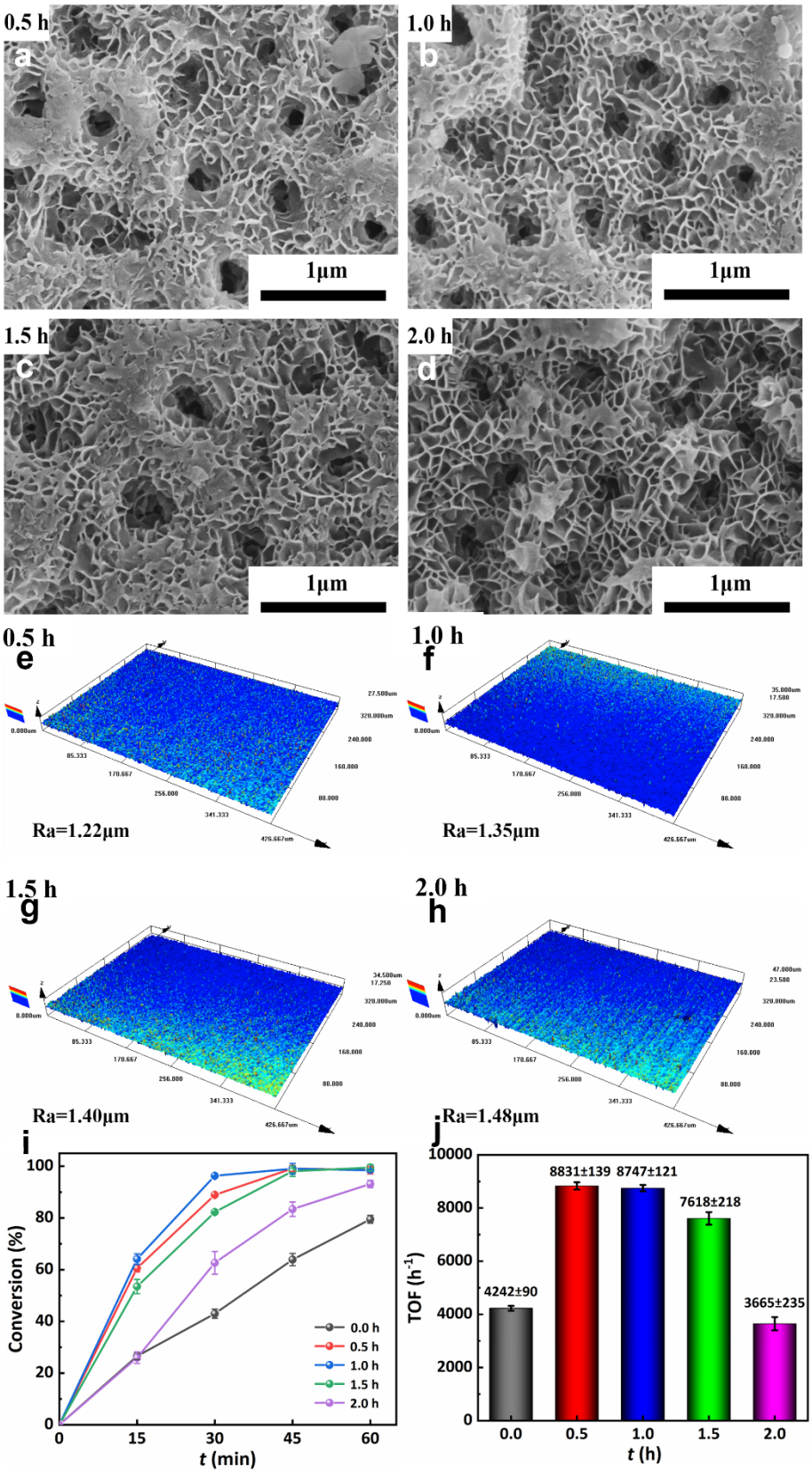

Figure S7 (a-h) Comparison of surface morphologies and roughness of Pd/MgO/Mg-2 after etching with different time; (i) Catalytic conversion; (k) TOF *vs* time.

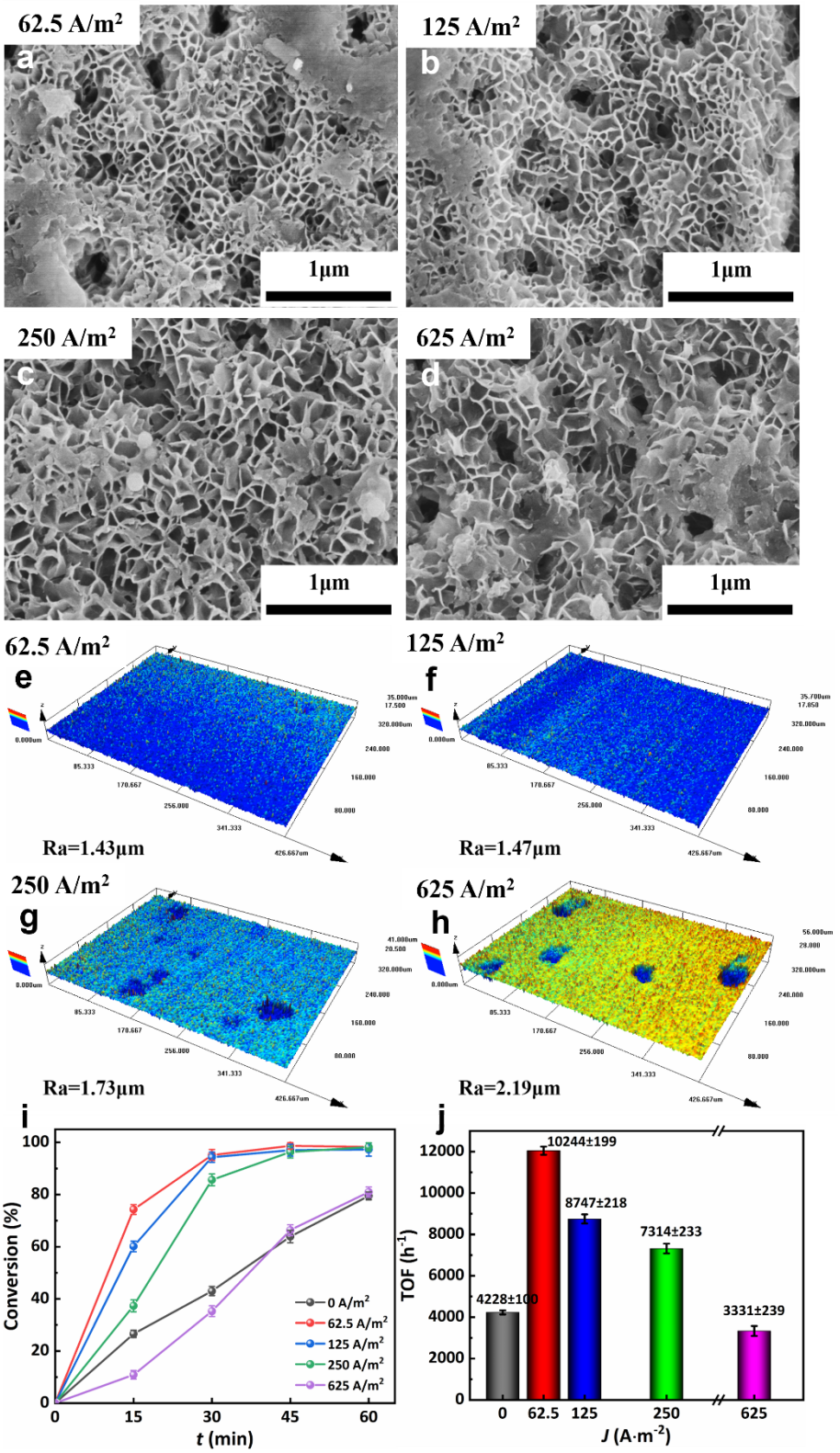

Figure S8 Comparison of surface morphologies and roughness of Pd/MgO/Mg-2 after etching with different currents; (i) Catalytic conversion; (k) TOF *vs* current.

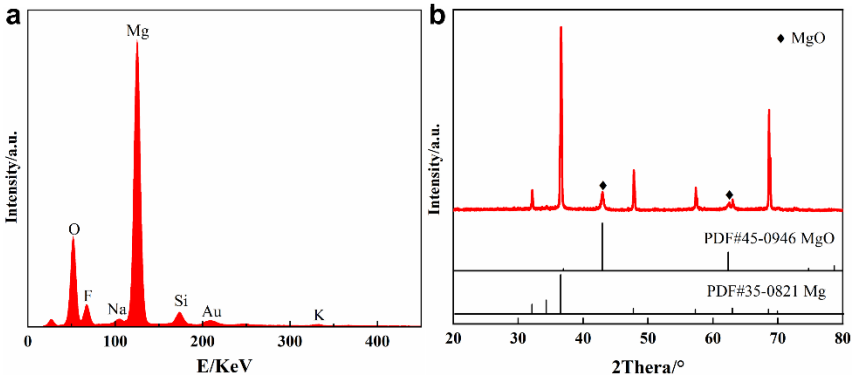

Figure S9 Component analysis of Pd/MgO/MgO-2 catalyst. (a) EDS energy spectrum; (b) XRD spectrum.

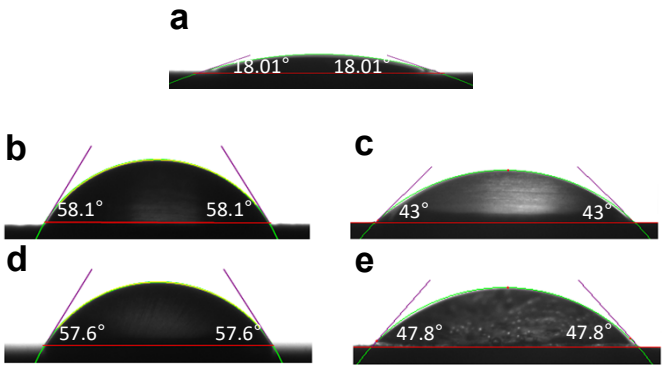

Figure S10 Water contact angle of the Pd/MgO/Mg-1 (original sample) and the Pd/MgO/Mg-2 (etched samples).(a) original Pd/MgO/Mg-1; (b) the optimal KNO_3 concentrations (0.2 mol/L); (c) the optimal electrolyte temperature (18℃); (d) the optimal etching times (1h); (e) the optimal etching currents(62.5 A/m^2).

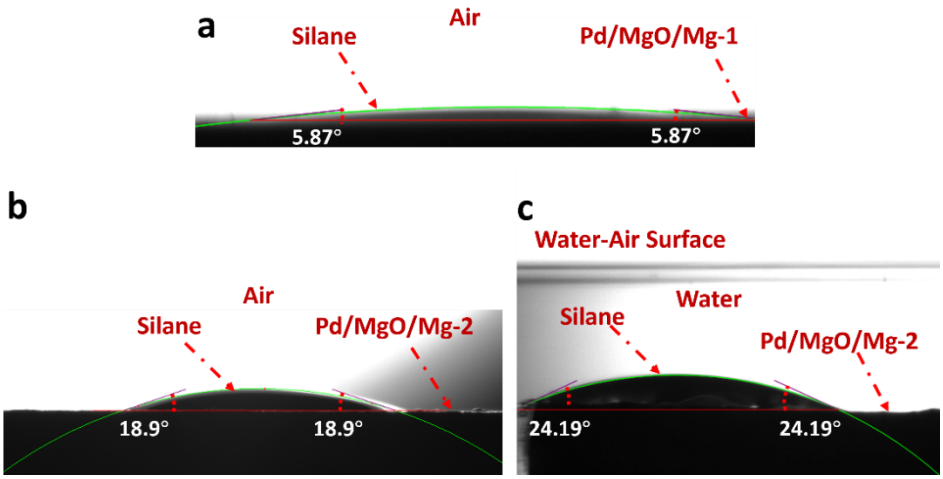

Figure S11 (a) Dimethylphenylsilane contact angle of the Pd/MgO/Mg-1 in air; (b) Dimethylphenylsilane contact angle of the Pd/MgO/Mg-2 in air; (c) Dimethylphenylsilane contact angle of the Pd/MgO/Mg-2 underwater.

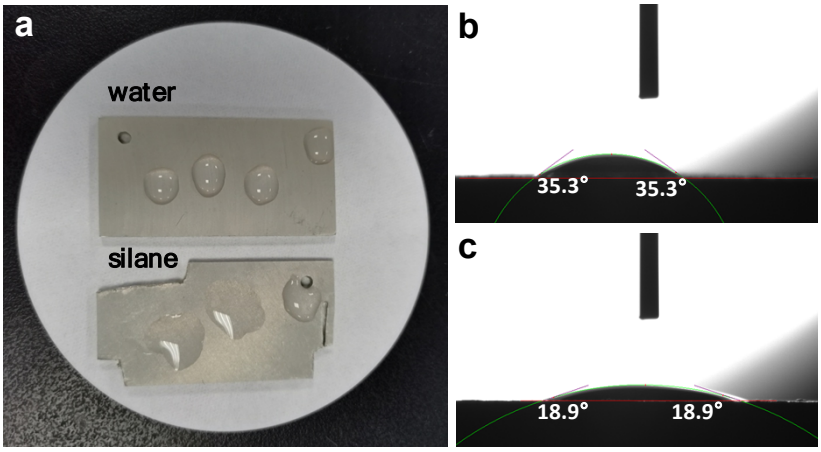

Figure S12 (a) Optical image of the water and silane drop on the Pd/MgO/Mg-2; (B) Water contact angle of the Pd/MgO/Mg-2; (c) Silane contact of the Pd/MgO/Mg-2.

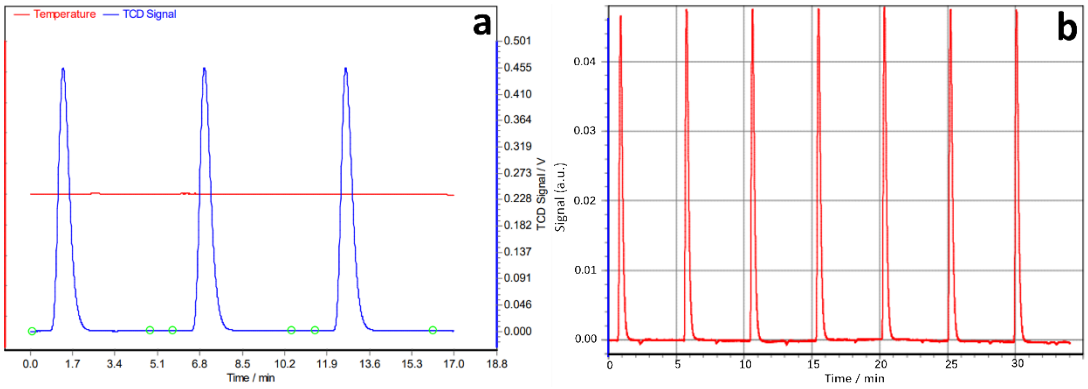

Figure S13 CO pulse chemisorption profiles of Pd/MgO/Mg catalysts. (a)Pd/MgO/Mg-1; (b)Pd/MgO/Mg-2.

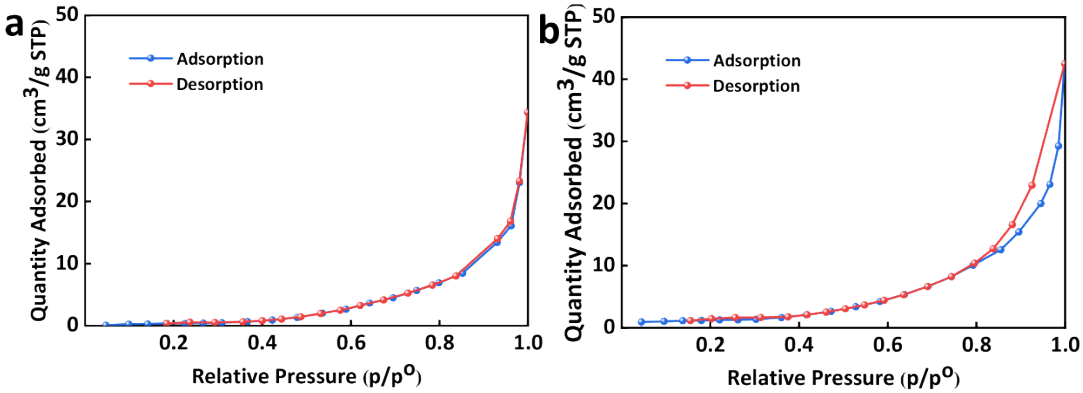

Figure S14 BET results of Pd/MgO /Mg catalysts. (a)Pd/MgO/Mg-1; (b)Pd/MgO/Mg-2.

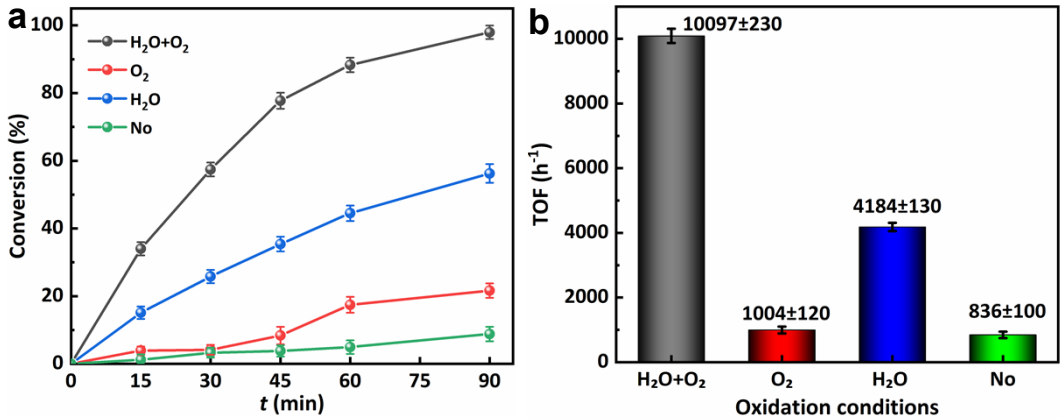

Figure S15 Effects of different oxidation conditions for the $PhMe_2SiH$ conversion with Pd/MgO/Mg-2. (a) conversion vs time; (b) TOF vs oxidation conditions.

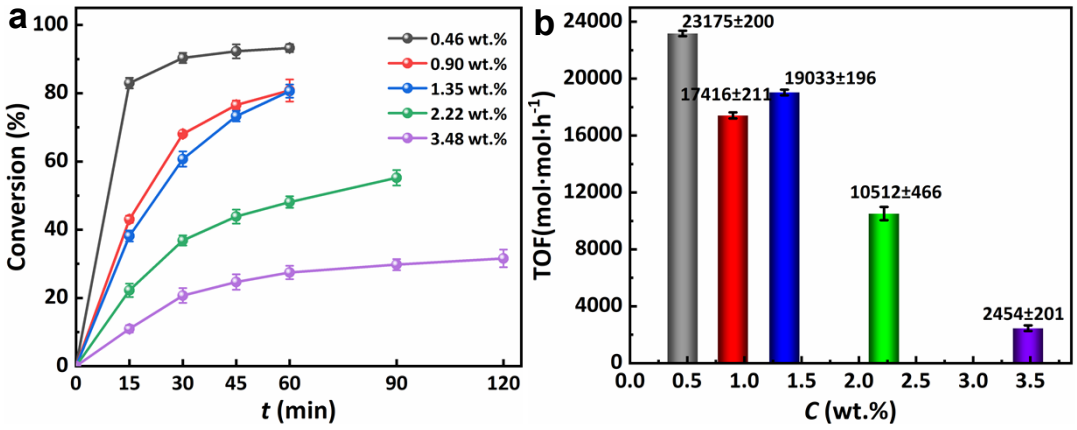

Figure S16 The optimal substrate concentrations with Pd/MgO/MgO-2 for the Et_3SiH conversion. (a) conversion vs time; (b) TOF vs mass fraction.

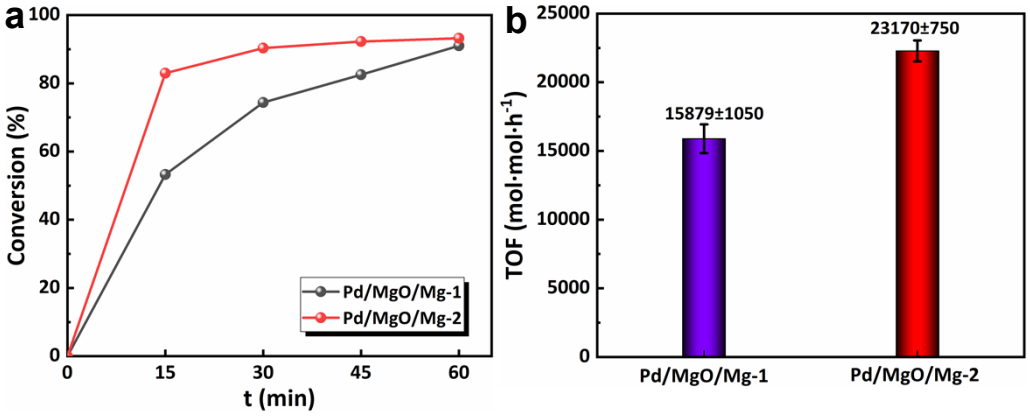

Figure S17 (a) The conversion rate of Et_3SiH with two Pd/MgO/Mg-1and Pd/MgO/Mg-2. (b) TOF of Et_3SiH conversion with two Pd/MgO/Mg catalysts.

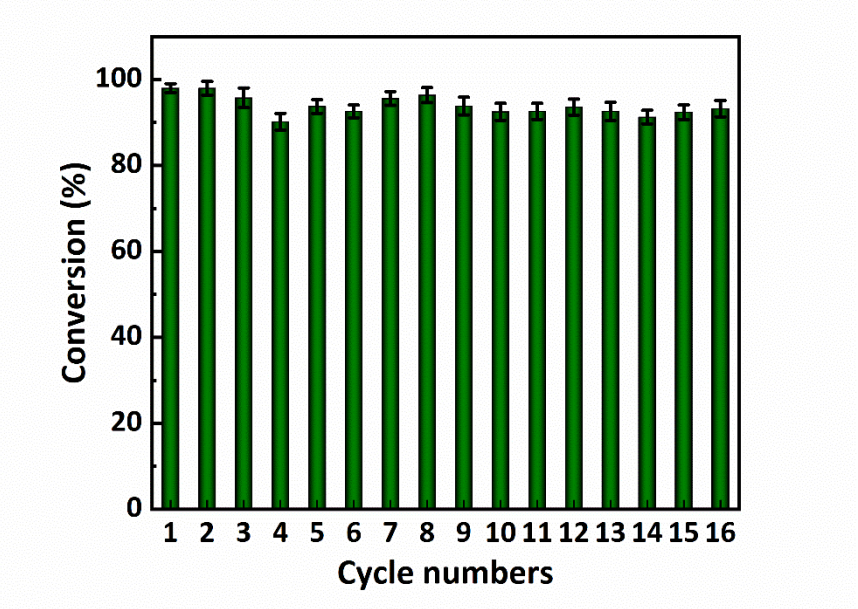

Figure S18 Cyclic stability of catalytic reactions for the Et_3SiH conversion with Pd/MgO/Mg-2 catalyst